Twenty-Sixth Symposium (International) on Combustion/The Combustion Institute, 1996/pp. 1137–1142

THE EFFECTS OF FLAME STRUCTURE ON EXTINCTION OF CH_4–O_2–N_2 DIFFUSION FLAMES

J. DU AND R. L. AXELBAUM
Department of Mechanical Engineering
Washington University
St. Louis, MO 63130

The effects of flame structure on the extinction limits of CH_4–O_2–N_2 counterflow diffusion flames were investigated experimentally and numerically by varying the stoichiometric mixture fraction Z_{st}. Z_{st} was varied by varying free-stream concentrations, while the adiabatic flame temperature T_{ad} was held fixed by maintaining a fixed amount of nitrogen at the flame. Z_{st} was varied between 0.055 (methane-air flame) and 0.78 (diluted-methane-oxygen flame). The experimental results yielded an extinction strain rate K_{ext} of 375 s^{-1} for the methane-air flame, increasing monotonically to 1042 s^{-1} for the diluted-methane-oxygen flame. Numerical results with a 58-step C1 mechanism yielded 494 s^{-1} and 1488 s^{-1}, respectively. The increase in K_{ext} with Z_{st} for a fixed T_{ad} is explained by the shift in the O_2 profile toward the region of maximum temperature and the subsequent increase in rates for chain-branching reactions. The flame temperature at extinction reached a minimum at $Z_{st} = 0.65$, where it was 200°C lower than that of the methane-air flame. This significant increase in resistance to extinction is seen to correspond to the condition in which the OH and O production zones are centered on the location of maximum temperature.

Introduction

Studies of strained laminar diffusion flames have proven useful, both for developing a fundamental understanding of flame structure and extinction and for application in the flamelet model of turbulent combustion. Flame extinction resulting from excessive strain is of particular importance and has received considerable attention. For a strained diffusion flame, Liñan's [1] results for one-step irreversible kinetics have shown that, for a given free-stream temperature, the oxidizer or fuel can leak through the flame. Which reactant leaks through depends on the ratio of oxidizer to fuel mass fractions. In the present work, the stoichiometric mixture fraction,

$$Z_{st} = (1 + Y_{F,\infty} W_O \nu_O / Y_{O,-\infty} W_F \nu_F)^{-1} \quad (1)$$

is used to characterize this ratio, where Y is the mass fraction, W is the molecular weight, ν is the stoichiometric coefficient, and the subscripts O and F refer to oxidizer and fuel, respectively. For $Z_{st} < 0.5$, oxidizer leaks through, whereas for $Z_{st} > 0.5$, fuel leaks through. A different reactant penetrates the flame with different Z_{st} because with one-step kinetics, the controlling feature for reactant leakage is the global structure of the flame, which is dictated only by the composition of the free-streams (assuming the temperatures of the free-streams are equal).

For the methane-air flame ($Z_{st} = 0.055$), it is well-known that oxygen leaks through the flame while methane is completely consumed [2]. One-step asymptotic analysis incorrectly predicts fuel leakage because, although the basic flame structure suggests fuel leakage, the rate-limiting oxidation kinetics result in oxygen leakage. Reduced mechanisms with two steps or more can capture separately the kinetics of fuel and oxygen consumption and thus predict oxygen leakage [2]. Although Liñan's results do not correctly identify which reactant leaks through the flame, they do demonstrate that extinction is intimately linked with outer flame structure, as dictated by Z_{st}, such that when the basic structure of the flame is altered, the extinction strain rate will be affected.

A common example of the effects of free-stream composition on extinction is the decrease in K_{ext} that occurs when reactants are diluted [3–5]. Fuel dilution decreases the flame temperature but also increases the stoichiometric mixture fraction, moving the flame away from the oxidizer and toward the fuel. The reduction in flame temperature slows chain branching while only weakly affecting radical recombination, making it easier to extinguish the flame. However, the basic structure also changes due to the shift in the flame location. To the best of the authors' knowledge, a systematic study of the effects of the shift in flame location on flame structure and extinction has not been performed.

Ishizuka and Tsuji [4] studied the effect of inert addition on extinction of methane flames. They diluted either the fuel or the air stream to determine the limiting fuel and oxidizer concentrations for stable burning. Their results showed that there is a

TABLE 1
Extinction Conditions for CH_4–O_2–N_2 Flames with T_{ad} = 2226 K.

	Flame A	Flame B	Flame C	Flame D	Flame E
Z_{st}	0.055	0.35	0.50	0.65	0.78
Y_{CH_4} at Z = 1	1.0	0.157	0.111	0.0845	0.0709
Y_{O_2} at Z = 0	0.233	0.339	0.437	0.632	1.0
K_{ext} (s^{-1}) (exp.)	375 ± 10	482 ± 10	601 ± 10	770 ± 20	1042 ± 20
K_{ext} (s^{-1}) (num.)	494	814	996	1226	1488
T_{ext} (K)	1770	1752	1651	1572	1656

limiting flame temperature that constrains the minimum concentrations for the reactants. Puri and Seshadri [3] studied the effects of dilution on propane as well as on methane flames. In this study, Z_{st} was held constant as oxygen mass fraction was varied to identify the extinction strain rate. A small range of Z_{st} was considered. Chen and Sohrab [5] also studied the limiting concentrations for methane flames and extended the study to include pure oxygen in the oxidizer, thus obtaining-limiting conditions under a wide range of fuel and oxidizer concentrations. In all of the mentioned studies, the free-stream compositions were varied with no attempt to maintain constant flame temperature. Thus, the extinction conditions observed are a consequence of changes in flame temperature and global structure.

The objective of this study is to identify the specific influence of flame structure (flame location) on extinction, and to this end, Z_{st} is varied while maintaining a constant adiabatic flame temperature. The extinction strain rates are obtained both experimentally and numerically. The experimental extinction strain rates serve to validate the numerical results, and the numerical results are then used to identify the structure and to explain the effects of Z_{st} on extinction.

This approach for studying the effects of Z_{st} at constant flame temperature has been employed by Du and Axelbaum [6] to understand the effects of structure on soot inception in ethylene flames. Lin and Faeth [7] have since employed this approach to experimentally study soot inception and flame extinction for a variety of fuels, and Sung et al. [8] followed this approach to understand the endothermic reactions on the fuel side of methane diffusion flames.

Experimental and Numerical Methodology

The experimental apparatus is described in detail in Du and Axelbaum [6]. Briefly, a flame is established between two 11-mm opposed jets spaced 8 mm apart. The jets emanate from tubes with honeycomb cores placed 50 cm upstream of each exit. An annular co-flow of nitrogen is added to both fuel and oxidizer to eliminate oxygen entrainment from ambient air and to extinguish the flame that would exist outside the region of interest. The complete flow field has not been characterized, but it is expected to be between potential and plug flow [9].

To obtain extinction strain rates, the flow rate is increased until extinction occurs. A bypass is used to ensure that the composition remains fixed as strain rate is increased. The flame is then reestablished at conditions very near extinction, and the velocity profile along the stagnation streamline is measured with laser-Doppler velocimetry. The strain rate, K, is identified as the magnitude of the slope of the velocity profile upstream of the flame. Because the densities of the fuel and oxidizer free-streams are similar, the velocity gradients on both sides of the flame are identical within experimental uncertainties.

The numerical scheme employed was developed by Smooke et al. [9]. The version of the code used here assumes that the flow field outside the mixing layer can be described by potential flow. The reaction mechanism used is the a 58-step C1 mechanism given in Ref. 10.

Results and Discussion

To study the effects of flame structure, Z_{st} must be varied while maintaining a constant adiabatic flame temperature. Z_{st} can be varied by simply adding inert to one of the reactants. However, as noted above, this will also change the flame temperature, and in this work, the objective is to isolate the effects of flame structure resulting from shifts in flame location. Therefore, our approach is to consider flames with different values of Z_{st} but with the same adiabatic flame temperature T_{ad}. To accomplish this, we start with the methane air flame as the reference condition. The stoichiometry is

$$CH_4 + 2O_2 + 7.52\,N_2 \rightarrow \text{products} \qquad (2)$$

The adiabatic flame temperature for this reaction is

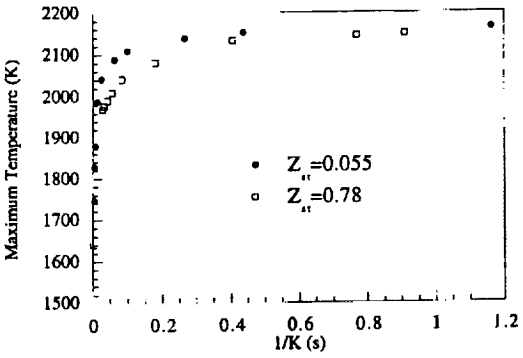

FIG. 1. Numerical results for maximum temperature as a function of $1/K$ for flames A (Z_{st} = 0.055) and E (Z_{st} = 0.78). For clarity, only select data are shown near K_{ext}.

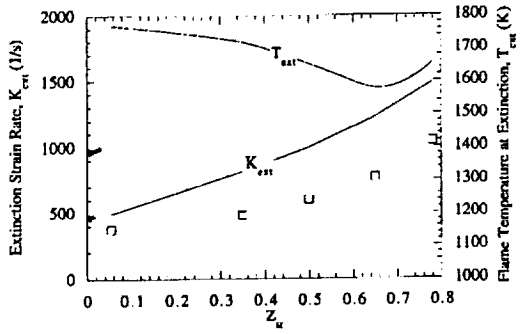

FIG. 2. Extinction strain rate and maximum temperature at extinction as functions of stoichiometric mixture fraction. Open squares denote experimental data for K_{ext}, and curves denote computational results.

2227 K. Z_{st} can be varied without changing T_{ad} simply by maintaining a fixed amount of nitrogen while varying the relative amount that is added to the fuel and oxidizer. Experimentally, this is accomplished by choosing flow rates that satisfy

$$Q_{N_2,O}/Q_O + Q_{N_2,F}/2Q_F = 3.76 \qquad (3)$$

where $Q_{N_2,i}$ is the flow rate of nitrogen mixed with the ith species, and subscripts O and F refer to O_2 and CH_4, respectively. To obtain the widest range of Z_{st} and thus more clearly delineate structural effects, flames are considered where all the nitrogen is introduced with the oxidizer (methane air flame, Z_{st} = 0.055) to the other extreme where it is introduced with the fuel, such that the oxidizer is pure oxygen (Z_{st} = 0.78).

The validity of this approach to maintaining constant flame temperature is demonstrated in Fig. 1, where the maximum temperature obtained from the numerical calculations is plotted as a function of $1/K$ for Z_{st} = 0.055 and for Z_{st} = 0.78. As $1/K \rightarrow \infty$, that is, in the limit of infinite Damköhler number, the temperatures of both flames asymptote to a common value, which is as expected because the adiabatic flame temperatures are the same. Nonetheless, the behaviors near extinction vary considerably. For low Z_{st}, the flame temperature is nearly constant until very close to extinction, where it abruptly falls off. For large Z_{st}, the temperature falls off much more gradually and persists to a much lower temperature. Though the fuel and T_{ad} are the same, the response of the flames to increasing K are very different.

The experimental extinction strain rates, averaged over five separate measurements, are listed in Table 1 for five different flames, flames A–E. For the methane air flame, K_{ext} = 375 s^{-1}, which is in good agreement with the results of Chelliah et al. [11], who found K_{ext} = 380 s^{-1}. The extinction strain rates are seen to increase with Z_{st}, even though T_{ad} is constant. For example, the strain rate required to extinguish the diluted methane-oxygen flame is almost three times as high as for the methane-air flame.

Table 1 also includes numerical results for K_{ext} and the flame temperature at extinction, T_{ext}. In Fig. 2, experimental and numerical results for K_{ext} are plotted as functions of Z_{st}. The numerical results are found to correctly predict the increase in K_{ext} with Z_{st}, yet they consistently overpredict K_{ext} by 30–50%. This discrepancy for the methane air flame has been observed by others and is due to the simplified kinetic scheme employed in the model and the assumption of potential flow outside the mixing layer, when the actual flow field is somewhere between potential and plug flow [11]. For the purposes of this study, a precise modeling of the flow field is not necessary and the potential flow assumption should be adequate. Thus, the qualitative agreement between experiment and theory over this wide range of Z_{st} demonstrates that C2 kinetics are not needed to predict the observed trends, and that the C1 scheme employed is sufficiently valid to allow it to be used to extract an understanding of how Z_{st} affects the structure of methane flames.

Before considering the results from detailed kinetics, it is instructive to evaluate how the outer structure of the flame is affected by increases in Z_{st} by considering a simple flame sheet argument. Since the adiabatic flame temperatures of flames A–E are the same, the primary effect of increasing Z_{st} is to shift the flame from the oxidizer toward the fuel. In doing so, the outer structure of the flame is affected. Considering the equilibrium (flame sheet) solution in Z space, shown in Fig. 3, the changes in outer structure are readily interpreted. For purposes of discussion, let T_{rb} represent a temperature that would define the boundaries of the reaction zone if the kinetics were finite. Noting the temperature profiles and the nominal boundaries of the *effective* reaction zone, it follows that for flame A, there is, on

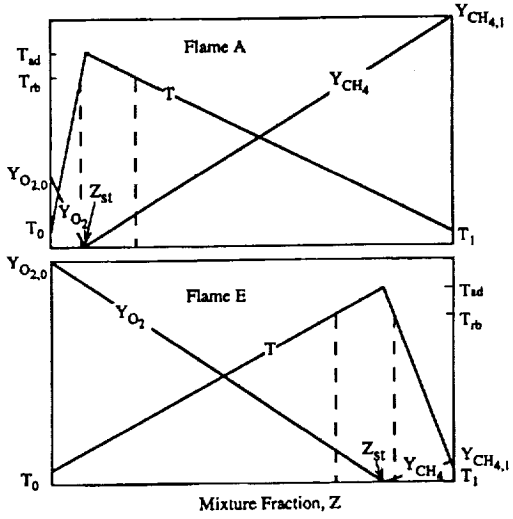

FIG. 3. Flame sheet solution for temperature and reactant profiles in Z space for flames A and E.

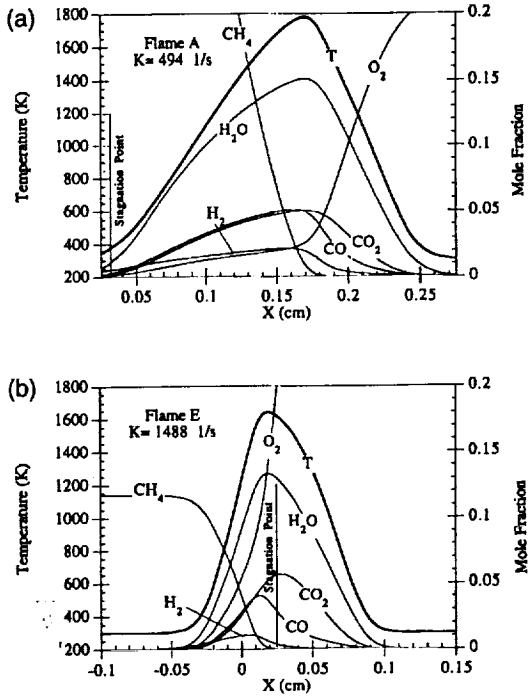

FIG. 5. Numerical results near extinction for major species profiles and temperature in the physical coordinate for (a) flame A, and (b) flame E.

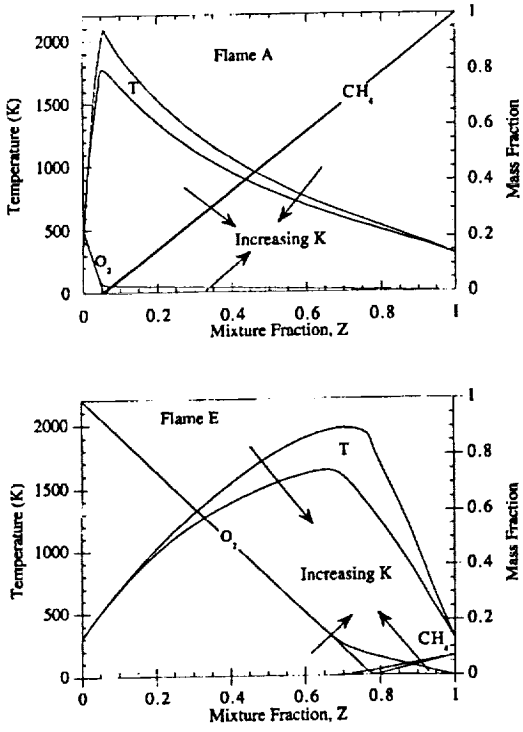

FIG. 4. Numerical results for methane, oxygen, and temperature profiles in Z space as functions of strain rate K for (a) flame A, and (b) flame E.

the average, more fuel than oxidizer in the high-temperature reaction zone for the low Z_{st} flame [2].

Now, considering flame E, which has the highest value of Z_{st}, it is clear that the average oxygen mass fraction within the reaction zone is much higher than that of flame A. The higher mass fraction within the high-temperature region of the flame would be expected to accelerate branching chemistry and produce more radicals. Thus, the flame would be stronger and more difficult to extinguish.

The validity of the preceding interpretation is confirmed by the numerical investigations employing detailed kinetics and transport properties. Figure 4 shows the reactant and temperature profiles obtained for flames A and E, plotted in mixture fraction space to allow for convenient comparison with Fig. 3. The high strain rate curves in Fig. 4 are at their corresponding extinction limits. These results show that oxygen leakage is common to all flames, as is the absence of methane leakage. Therefore, the oxygen consumption reactions are rate limiting at high Z_{st}, as they are for the methane air flame. Other than the increase in oxygen leakage, the methane and oxygen profiles are little affected by increasing strain rate. The temperature falls off, and the peak temperature shifts towards smaller Z.

Figure 5 shows the profiles of temperature and

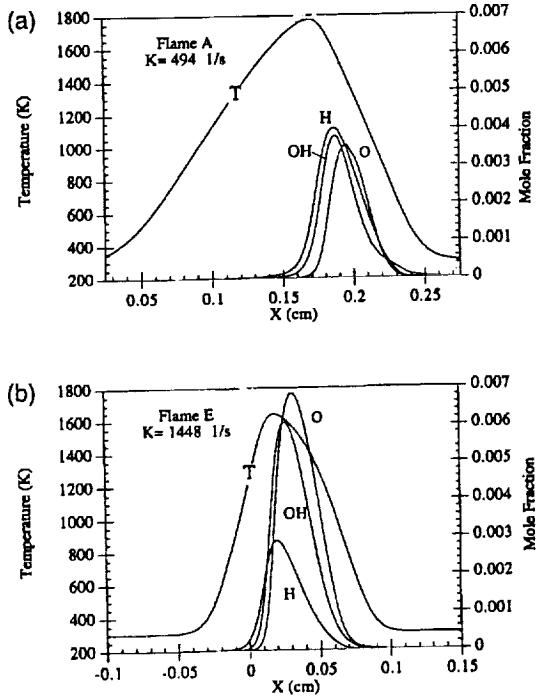

FIG. 6. Numerical results near extinction for profiles of OH, O, H, and temperature in the physical coordinate for (a) flame A, and (b) flame E.

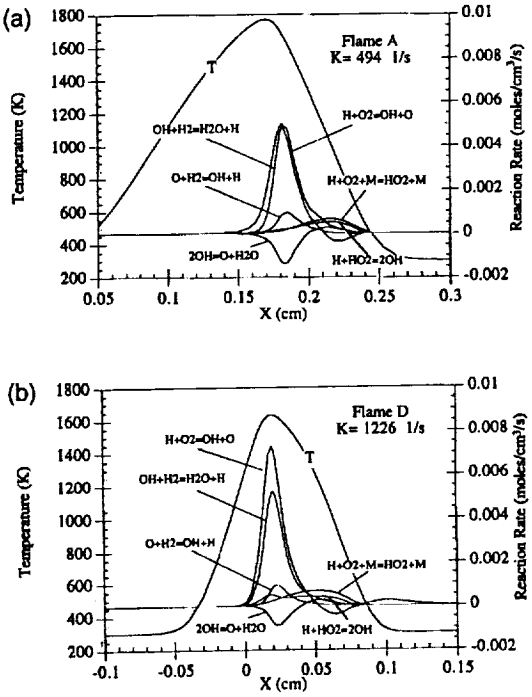

FIG. 7. Reaction rate profiles for the primary radical production reactions and temperature in the physical coordinate for (a) flame A, and (b) flame D.

major species for conditions near extinction in the physical coordinate for flames A and E, with the location of the stagnation point shown for reference. As Z_{st} increases, the flame location moves toward the stagnation point, with flame C (Z_{st} = 0.5) being located approximately at the stagnation point. With further increases in Z_{st}, the flame location moves past the stagnation point toward the fuel boundary. In addition, the amount of oxygen in the high-temperature region increases as Z_{st} increases. For example, at T = 1600 K on the oxidizer side, there is 5.7 mole % O_2 for flame A as compared to 23.0 mole % for flame E. Thus, these findings are consistent with the flame sheet arguments described previously.

The amount of fuel in the high-temperature zone is considerably greater in flame A than in flame E. Although the rate of fuel pyrolysis is not expected to have a dominant effect on flame extinction, this finding does have important implications for soot formation; and in Ref. 6, the effects of flame structure on soot formation have been discussed.

In Fig. 6, the profiles of O, H, and OH near extinction are shown for flames A and E. The concentrations of OH and O are higher in flames with higher Z_{st}, whereas those of H are somewhat lower. The combination of high temperature and large oxygen concentration in the vicinity of the hydrogen radical pool accelerates the primary chain branching reaction,

$$H + O_2 \rightarrow OH + O \qquad (4)$$

because this reaction has a high activation energy and is first order in O_2 concentration. Thus, higher Z_{st} favors production of OH and O and consumption of H. Numerical results for flames with $K = 1/2K_{ext}$ have also been obtained to ensure that the given trends are not anomalies associated with the unstable conditions at extinction. Though the radical pool increases when K is decreased, the trends are consistent with those of Fig. 6 and lead to the same conclusions as to the effects of Z_{st}.

The Z_{st} = 0.78 flame can withstand a lower temperature before extinction because the increases in OH and O provide greater resistance to extinction, allowing the flame temperature at extinction T_{ext} to be lower. As shown in Fig. 2, the dependence of T_{ext} on Z_{st} is not monotonic. T_{ext} approaches a minimum of 1299°C near Z_{st} = 0.65 (flame D), which is 200°C lower than for the methane-air flame. Figure 7, which is a plot of rates for the radical production reactions for flames A and D, suggests an explanation for this behavior. The reaction rates for these reactions, particularly Eq. (4), are centered at the

location of maximum temperature for flame D, whereas they are far from this location for flame A. Thus, the temperature where the hydroxide and oxygen radicals are produced is comparable to the flame temperature for flame D, as opposed to about 100°C less for flame A. Consequently, the flame temperature can be reduced more for flame D than for flame A before the temperature in the radical production zone is reduced to an extent that the flame can no longer support combustion. For $Z_{st} > 0.65$, the radical production zone is shifted farther toward the fuel, and the maximum temperature must again be higher to sustain radical production.

Conclusions

For the CH_4–O_2–N_2 system at a given adiabatic flame temperature, the extinction limits increase with stoichiometric mixture fraction. This increase, which results from the shift in the O_2 profile into regions of higher temperature, raises the OH and O production rates and concentrations in this region, yielding stronger flames. This shift in the relative temperature and O_2 profiles also results in a difference of up to 200°C in the extinction temperature for the same fuel and the same adiabatic flame temperature. This result is contrary to what is suggested from the data of Ishizuka and Tsuji [4], that there is a unique limit temperature that constrains the extent of dilution that a flame can sustain. The position of the radical production zone relative to the maximum temperature appears to be critical in identifying the limit temperature for stable burning.

The results of this study are also relevant to practical flames wherein the fuel is diluted and/or the oxidizer is enriched. There are a number of applications where enriched oxygen is presently used, notably in blast furnaces. Enriched oxygen combustion has also been proposed to reduce particulates, for example, in diesel engines [12].

REFERENCES

1. Liñán, A., *Acta Astronautica*, 1:1007–1039 (1974).
2. Williams, F. A., *Reduced Kinetic Mechanisms and Asymptotics Approximations for Methane-Air Flames* (Smooke, M. D., Ed.), Springer Verlag, New York, 1991.
3. Puri, I. K. and Seshadri, K., *Combust. Flame* 65:137–150 (1986).
4. Ishizuka, S. and Tsuji, H., *Eighteenth Symposium (International) on Combustion*, The Combustion Institute, Pittsburgh, 1981, pp. 695–703.
5. Chen, C. L. and Sohrab, S. H., *Combust. Flame* 86:383–393 (1991).
6. Du, J. and Axelbaum, R. L., *Combust. Flame* 100:367–375 (1995).
7. Lin, K. C. and Faeth, G. M., *Propulsion Power* 12(4):691–698 (1996).
8. Sung, C. J., Liu, J. B., and Law, C. K., *Combust. Flame* 102:481–492 (1995).
9. Smooke, M. D., Puri, I. K., and Seshadri, K., *Twenty-First Symposium (International) on Combustion*, The Combustion Institute, Pittsburgh, 1986, pp. 1783–1792.
10. Bilger, R. W., Starner, S. H., and Kee, R. J., *Combust. Flame* 80:135 (1990).
11. Chelliah, H. K., Law, C. K., Ueda, T., Smooke, M. D., and Williams, F. A., *Twenty-Third Symposium (International) on Combustion*, The Combustion Institute, Pittsburgh, 1990, pp. 503–511.
12. Sekar, R. R., Marr, W. W., Assanis, D. N., Cole, R. L., Marciniak, T. J., and Schaus, J. E., *J. Eng. Gas Turbines Power* 113:365–369 (1991).